ADVANCES IN ATMOSPHERIC SCIENCES, VOL. 21, NO. 5, 2004, 717–729

Using a Modified Soil-Plant-Atmosphere Scheme (MSPAS) to Study the Sensitivity of Land Surface and Boundary Layer Processes to Soil and Vegetation Conditions

LIU Shuhua*[1,2] (刘树华), YUE Xu[1] (乐 旭), LIU Huizhi[2] (刘辉志), and HU Fei[2](胡 非)

[1] *Group of Atmosphere Boundary Layer and Turbulence, Laboratory of Severe Storm Research, Department of Atmospheric Sciences, the College of Physics, Peking University, Beijing* 100871

[2] *State Key Laboratory of Atmosphere Physics and Chemistry, Institute of Atmospheric Physics, Chinese Academy of Sciences, Beijing* 100029

(Received 8 May 2003; revised 3 September 2003)

ABSTRACT

A series of sensitivity tests are performed to test the stability and sensibility of the Modified Soil-Plant-Atmosphere Scheme (MSPAS), which was wholly introduced in a previous paper. The numerical simulation results from the experiments show good agreement with physical reality. Besides, some of the results are illuminating. Together with the first paper, it is concluded that MSPAS is a simple but effective model, and it is practically valuable in the research work of desertification control and reforestation in China

Key words: Modified Soil-Plant-Atmosphere Scheme, desertification, sensitivity test

1. Introduction

In our previous paper, MSPAS (Modified Soil-Plant-Atmosphere Scheme) was fully introduced and the effectiveness of the model was also well proved (Liu et al., 2004). In this paper, some sensitivity experiments are performed to test the stability and sensibility of the model, which are important indexes for a model.

A further significance of this paper is its contribution to the desertification control of China. As we know, desertification is a serious problem in China. According to the definition given in the UN (United Nation) Convention for Combating Desertification, 34.6% of the national total land area is affected by desertification, which greatly hinders social-economic development and environmental protection (Wu and Lu, 2002).

In the 1980s, two important models (BATS, Dickinson et al., 1986; Dickinson et al., 1993; and SiB, Sellers et al., 1986, 1996) were developed based on detailed considerations of the importance of vegetation in the land surface interaction. From some sensitivity experiments of the two models by considering the effects of vegetation, more realistic results can be obtained in calculating the fluxes. In the SiB model, the main method for considering the effect of vegetation is to mimic the biosphere and physiological process in the vegetation, and to make the vegetation decide the interactions between the surfaces and the atmosphere. The SiB model was developed over a dense and tall vegetated surface. Because of the simple water and heat transfer scheme in the soil, it cannot be used in semi-arid areas or deserts (Clapp, 1978).

Charney et al. (1977) studied the influence of the variation of the surface reflective index on climate, finding that it has an important influence on the climate in arid areas. Mahfouf et al. (1987) studied the influences of soil and vegetation on the development of mesoscale circulation.

Bhumralkar (1975) and Blackadar (1976) proposed a 12-layer model in the predicting of ground surface temperature, which obtained perfect results against experiments. As a milestone, Deardorff's (1978) research work proved that sound results could be obtained by a simpler simulation. In his paper, he compared five approximate methods in predicting ground surface temperature with the 12-layer soil model. Noilhan and Planton (1989) proposed the most effective

*E-mail: lshuhua@pku.edu.cn

simulation method of the time. They continued to use the same method as Deardorff (1978) in the prediction of ground surface temperature and moisture content. However, they greatly inproved the parameterization of vegetation, which enhanced the precision in calculating specific humidity on the ground and made the computation more physically reasonable. The feasibility of this model was approved by Sang and Wu (1992) and Liu et al., (1997, 2002). Bonan and Land (1996) developed a surface model (LSM Version 1.0) for ecological, hydrological, and atmospheric studies. Sellers et al. (1996) gave a land surface parameterization (SiB2) for atmospheric GCMs.

Sun and Xue (2001) developed a new snow scheme in a simplified simple biosphere model and tested it against field data from Russia and France. The relevant equations in the scheme were given, which describe complicated interactive processes among the air-vegetation-snow-soil continuum through mass and heat exchange. The numerical results from the scheme show good agreement with field data. This indicates that the scheme they developed is workable and can be extended for climate study. Guo et al. (2002) presented the statistical relationship between soil thermal anomaly and short-term climate change based on a typical case study. Furthermore, possible physical mechanisms behind the relationship were revealed through an off-line land surface model with a reasonable soil thermal forcing at the bottom of the soil layer. Zhang and Lu (2002) developed a simple frozen soil parameterization scheme based on NCAR LSM and the effects of the revised scheme were investigated using measurement data from six stations of the Former Soviet Union (FSU). Dan et al. (2002) gave an atmosphere-vegetation interaction model (AVIM) coupled with a 9-layer general circulation model (GCM) of State Key Laboratory of Numerical Modeling for Atmospheric Sciences and Geophysical Fluid Dynamics/Institute of Atmospheric Physics, Chinese Academy of Sciences (LASG/IAP-CAS), which is rhomboidally truncated at zonal wave number 15, to simulate global climatic mean states. The work created a solid base for coupling a regional climate model with the biosphere.

Today, desertification control is of great importance in narrowing the gap between the east and the west. In this paper, the results of several sensitivity tests quantitatively reveal the important role that vegetation plays in the stability of regional climate, which are useful guides in the reforestation work in China.

Because the previous paper introduced the model in detail, and since all the sensitivity experiments appearing in this paper are mainly concerned with vegetation fraction $\sigma_{\rm f}$, albedos $\alpha_{\rm f}, \alpha_{\rm g}$, and soil water content $w_{\rm g}, w_2$, which means that changes to the model are minimal, we therefore defer discussion of the numerical model and parameterization, and of the difference scheme and initial and boundary conditions to the first paper, and proceed directly to results and analyses. In sections 2.1 and 2.2, we reanalyze some experiments done by Deardorff (1978) for their significance in the land surface processes and values in our conclusions for desertification control. And in section 2.3, we design six experiments to purposely find the dominant factor among the main physical variables. Interesting and valuable results are discussed in the following paragraphs (since all the variables have appeared in our last paper, we just list them in the appendix).

2. Results and analyses

2.1 *Influence of vegetation fraction on the land surface physical process*

As we know, the fraction of vegetation covering on the ground greatly influences energy budget between the land surface and atmosphere. In this part, an experiment is designed to testify this point of view, meanwhile to quantify such influence. The total time for the simulation is two days with a first 24-hour period begining at 18:00 (all times are local). A second 24-hour period follows, with the same conditions as those of the first, except for the simulation of 2-cm of rainfall between 18:00 and 22:00. The step for our calculations is 10 seconds. The following discussion will focus on two specific aspects: temperature and water content in the soil.

Figure 1 shows the diurnal variation of $T_{\rm g}$ (temperature of the ground) with different vegetation factor $\sigma_{\rm f}$. As it indicates, the greater the vegetation cover, the cooler in the daytime and warmer at night the land surface will be. These results due to the shelter provided by the plants which insulates land from the radiation of the Sun and protects the heat flux of the soil from a great loss after sunset.

Another comparison of the curves shows that plants do good to the stability of the climate in a region, because we can find that the maximum bare ground temperature is lower on the second day than on the first day because of the effect of the simulated rainfall during the intervening evening. However, this kind of change is not obvious for the land that covered by plants. This function of plants suggests that the development of virescence or reforestation is of great importance in improving of the stability of regional climate. This point of view will be confirmed again and again later in the paper by different ways.

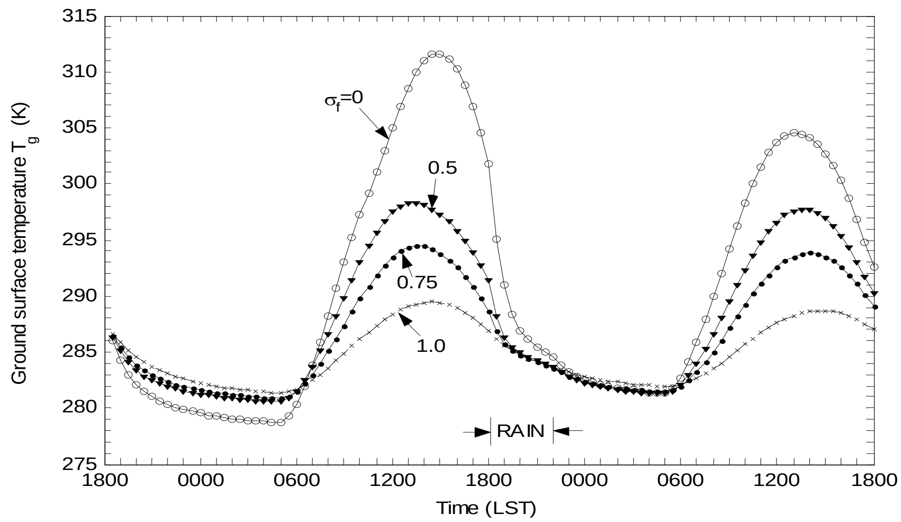

Fig. 1. Variation of the ground surface temperature with different vegetation fractions calculated by the model over a 2-day period.

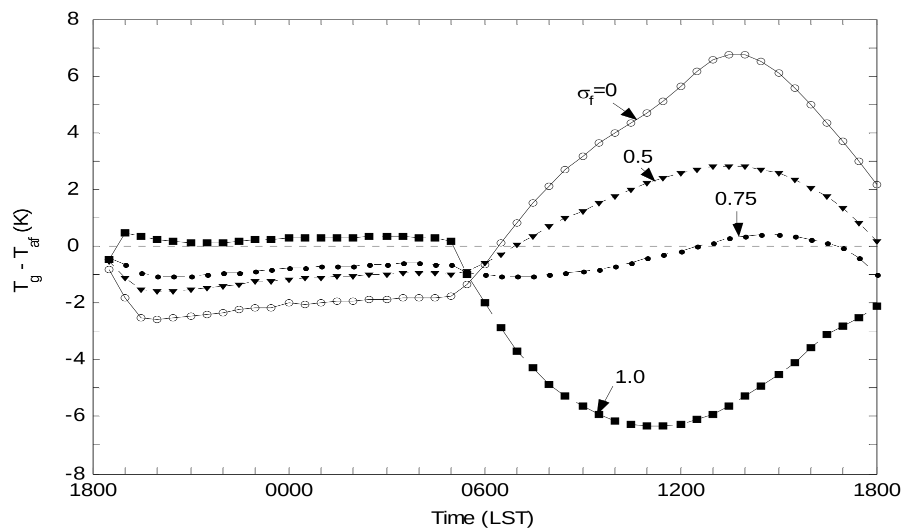

Fig. 2. Variation of T_g–T_{af} with different vegetation fractions during the 24-hour period calculated by the model.

A comparison between T_g and T_{af} (temperature of the atmosphere within canopy) is also conducted, and their difference is showed in Fig. 2. When considering bare ground ($\sigma_f = 0$), we see that the value of $T_g - T_{af}$ is positive in the daytime and negative at night; that is to say, the sensible heat flux from the land surface is upward in the daytime and becomes downward at night. While the tendency of curve is coming to the opposite side as the vegetation fraction grows. For example, in the dense canopy ($\sigma_f = 1.0$), the ground temperature is lower than the atmosphere in the canopy during daytime. That is because foliage prevents much of radiation from coming to the ground, resulting in little increase of T_g.

Now, let us look at the variation of water volume fraction in the soil. The vegetation fraction changes from 0 to 1, and corresponding changes occur in w_g (volume fraction of soil moisture on the ground) as showed in Fig. 3. We can see that compared with the land covered with plants, w_g of bare ground reduces quickly after the sun rises because of the lack of protection which would help preserve soil moisture. On the other hand, the dense canopy ($\sigma_f = 1.0$) causes the increase of w_g, no matter how intense the sunshine. Besides, the fluctuation is much smaller than the former situation. This special function of plants suggests that vegetation plays an important role in preserving soil moisture, and the denser the vegetation is the better effect it contributes.

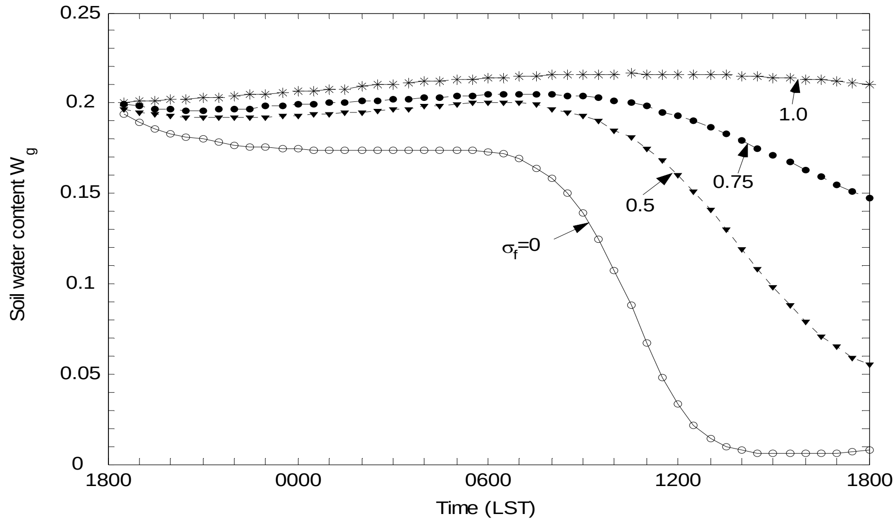

Fig. 3. Variation of water fraction in soil, w_{g}, in a day according to different vegetation fractions.

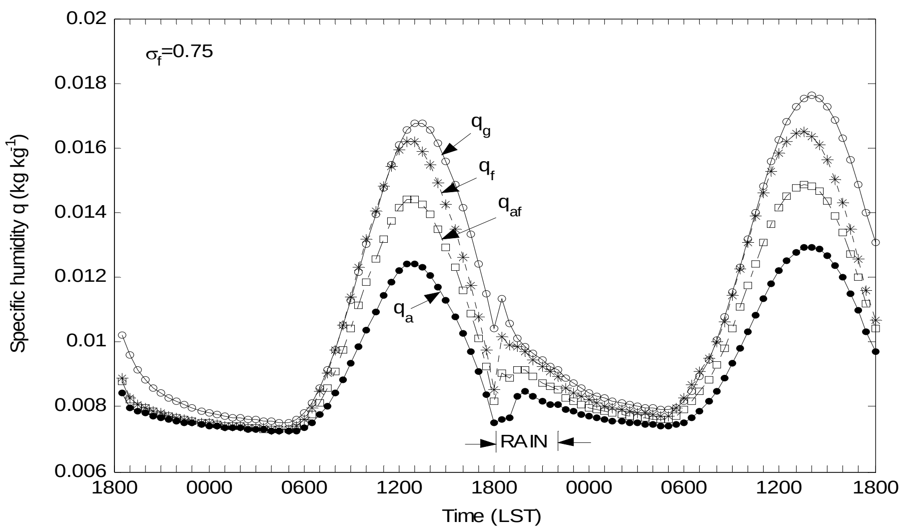

Fig. 4. Variation of $q_{\mathrm{f}}, q_{\mathrm{af}}, q_{\mathrm{g}}$, and q_{a} over the 2-day period for a shielding factor of 0.75 ($\sigma_f = 0.75$).

2.2 *Studies on the effect of rainfall*

In our simulation, we have designed a 'manual rain' during a specific period as described above, whose influence will be discussed in this part.

The most obvious contribution brought about by rain is the increase of water, no matter the liquid form as dew intercepted by the foliage or gas form as specific humidity diffusing in space. Figures 4 and 5 show such changes. Figure 4 records the variation of predicated specific humidity $q_{\mathrm{a}}, q_{\mathrm{g}}, q_{\mathrm{af}}$, and q_{f} throughout the 2-day period with the simulated rain taking place from 18:00 to 22:00 on the second day. q_{g} is the biggest one among those four variables. This is partially because of the initial value we set for the calculations. However, the most central reason is that the vapor from the soil is more than that from the foliage. This property of moisture does not change no matter in the daytime or at night until the rain comes. In Fig. 4, we can clearly see the increases of all four variables, among which q_{f} plays the most conspicuous role. During the period of rain, much water is intercepted by the foliage, which leads to increasing greatly. However, the normal relationship comes back shortly after the rain stops, accompanied by the rise of the maxima of the four humidity terms.

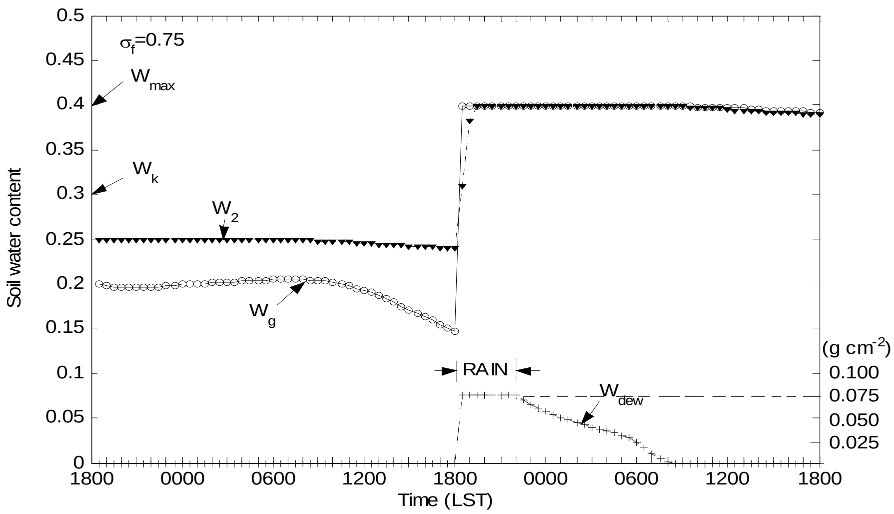

Fig. 5. Predicted variation of surface ($w_{\rm g}$) and bulk (w_2) soil moisture and of ($W_{\rm dew}$) (right-hand scale) over the 2-day period for $\sigma_f = 0.75$.

Figure 5 reveals such changes in another way w_g. represents the volume fraction of water contented in the topsoil, which contributes most to $q_{\rm g}$. Before the rain, $w_{\rm g}$ decreases after the Sun rises, which explains why $q_{\rm g}$ is the top one among the other specific humidities. When the rain falls on the ground, $W_{\rm dew}$ (interception of water on the foliage when raining) reaches a maximum value quickly because of the high ratio of vegetation cover. As we know, dew on foliage will surely increase the ambient specific humidity; that is to say, $q_{\rm f}$ increases greatly. When the rain stops, most of the dew falls on the ground and everything comes back to normal. All of the processes are just the same as what has been described in the above passage.

Another change brought about by the rainfall is revealed by Fig. 1. As it shows, the temperature at night on the ground surface increases compared with the same time during the first day. This change indicates the warming effect caused by overcast sky is greater than the cooling effect caused by rainwater. This is congruent with our life experience and plays an important role in agriculture.

2.3 *Additional sensitivity experiments*

We have discussed the influence of the vegetation fraction on the variation of some physical variables in section 2.1. In fact, besides $\sigma_{\rm f}$, there are some other parameters whose variation could more or less cause a change in the environment, such as albedo, soil water content, and so on. In this part, some sensitivity experiments will be conducted to test which parameter is dominant in the determination of a physical variable. The meanings of all variables are explained in the appendix.

Table 1. Parameters set in the sensitivity experiments.

NO.	$\sigma_{\rm f}$	$\alpha_{\rm f}$	$\alpha_{\rm g}$	$w_{\rm g}$	w_2	$w_{\rm k}$
1	0.75	0.20	$\alpha_{\rm g} = 0.31 - 0.17 w_{\rm g}/w_{\rm k}$ $(w_{\rm g} \leqslant w_{\rm k})$ $\alpha_{\rm g} = 0.14$ $(w_{\rm g} > w_{\rm k})$	0.20	0.25	0.30
2	0.60	0.24	$\alpha_{\rm g} = 0.37 - 0.20 w_{\rm g}/w_{\rm k}$ $(w_{\rm g} \leqslant w_{\rm k})$ $\alpha_{\rm g} = 0.17$ $(w_{\rm g} > w_{\rm k})$	0.20	0.25	0.30
3	0.60	0.20	$\alpha_{\rm g} = 0.31 - 0.17 w_{\rm g}/w_{\rm k}$ $(w_{\rm g} \leqslant w_{\rm k})$ $\alpha_{\rm g} = 0.14$ $(w_{\rm g} > w_{\rm k})$	0.24	0.30	0.36
4	0.45	0.24	$\alpha_{\rm g} = 0.37 - 0.20 w_{\rm g}/w_{\rm k}$ $(w_{\rm g} \leqslant w_{\rm k})$ $\alpha_{\rm g} = 0.17$ $(w_{\rm g} > w_{\rm k})$	0.24	0.30	0.36
5	0.90	0.20	$\alpha_{\rm g} = 0.31 - 0.17 w_{\rm g}/w_{\rm k}$ $(w_{\rm g} \leqslant w_{\rm k})$ $\alpha_{\rm g} = 0.14$ $(w_{\rm g} > w_{\rm k})$	0.20	0.25	0.30
6	0.20	0.20	$\alpha_{\rm g} = 0.31 - 0.17 w_{\rm g}/w_{\rm k}$ $(w_{\rm g} \leqslant w_{\rm k})$ $\alpha_{\rm g} = 0.14$ $(w_{\rm g} > w_{\rm k})$	0.20	0.25	0.30

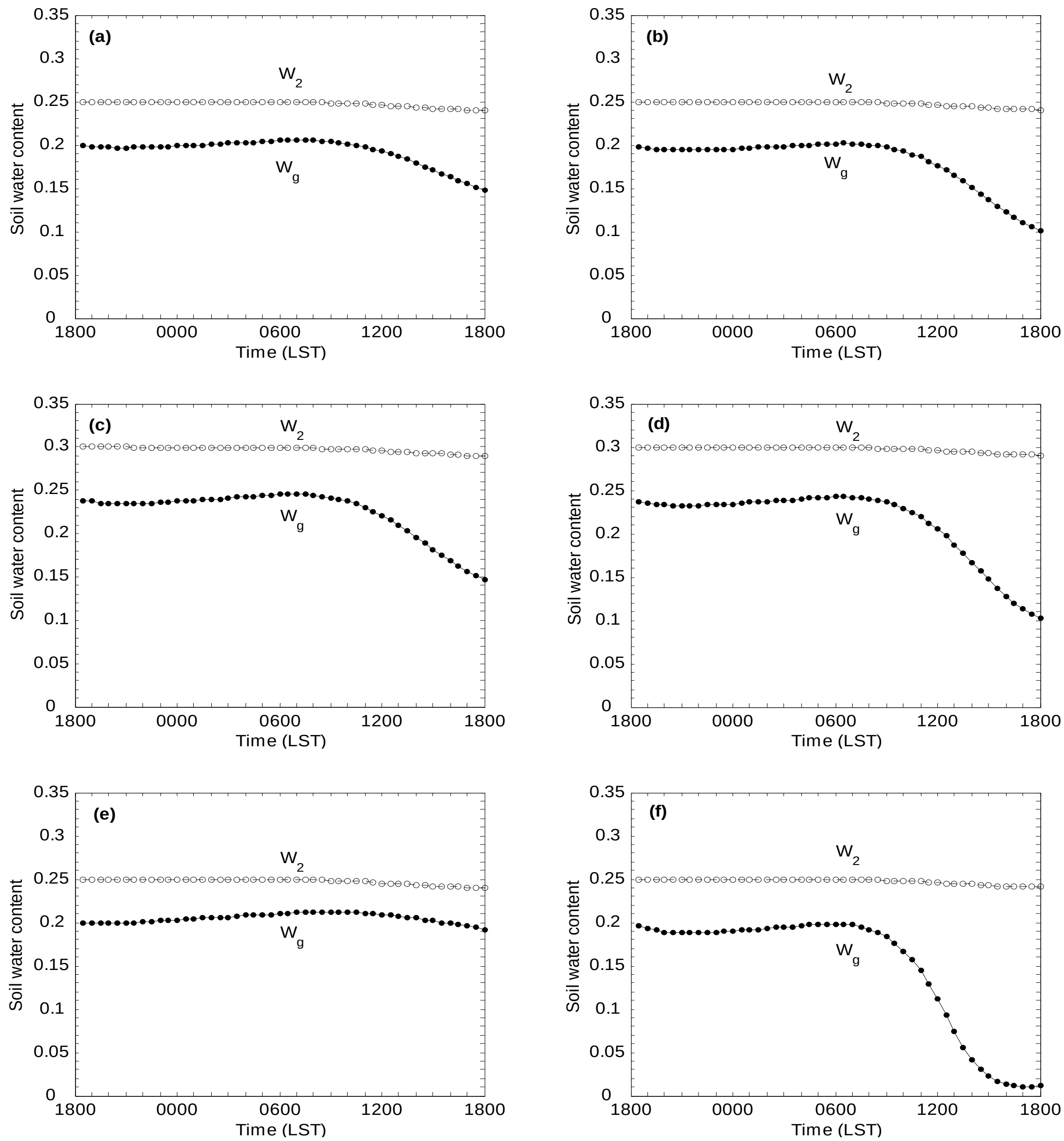

Fig. 6. Variation of soil water content in sensitivity experiments. (a) Expt. 1, (b) Expt. 2, (c) Expt. 3, (d) Expt. 4, (e) Expt. 5, and (f) Expt. 6.

The specific parameters in our experiments are listed in Table 1, which are designed intentionally rather than randomly. We take the first experiment as our reference, and the others are changed regularly. In the second experiment, vegetation factor reduces by 20%, meanwhile, its albedo increase by 20%. In the third experiment, vegetation factor still reduces by 20% and soil water content increase by 20% instead of albedo. In the fourth experiment, σ_{f} decreases by 40%, and both albedo and soil water content increase by 20%. The last two experiments is designed only to test influence of vegetation fraction variation, so one is up to 0.9 with the other down to 0.2.

Figure 6 variation of soil water content in our sensitivity experiments. We still take the result of the first experiment as reference. The variation of w_{g} in Expt. 2 is larger than that in Expt. 1, which shows that σ_{f} is much more important in controlling the soil water fraction than α_{g} and α_{f}. In the same way, we find that the vegetation factor plays a dominant role compared with the initial value of w_{g}, w_2 and w_{k} from Expt. 3. Experiment 4 approves this point of view by showing that the effect of σ_{f} exceeds the total effect of albedo and soil water content. Experiment 5 tells us that soil

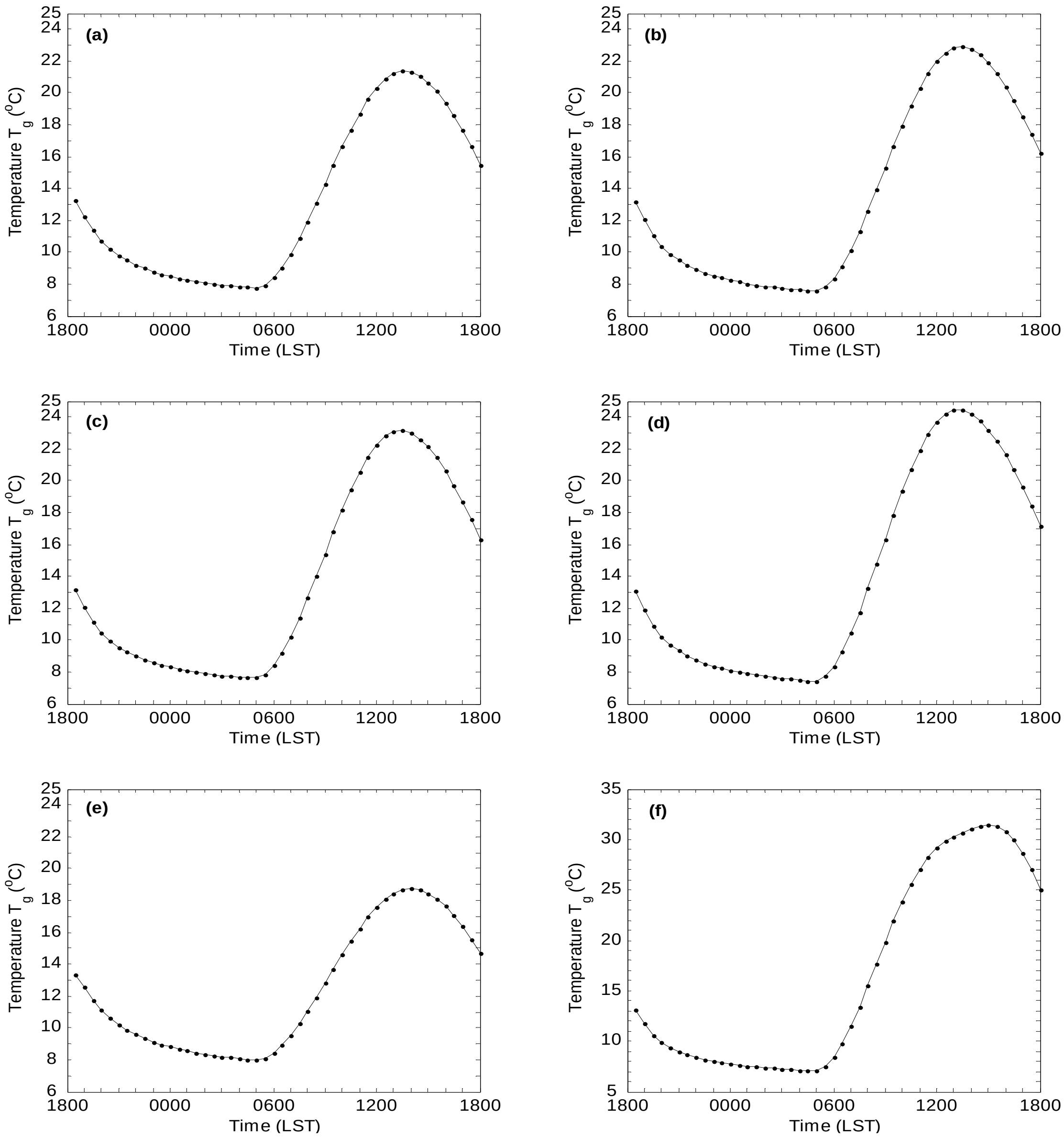

Fig. 7. Variation of ground surface temperature in sensitivity experiments. (a) Expt. 1, (b) Expt. 2, (c) Expt. 3, (d) Expt. 4, (e) Expt. 5, and (f) Expt. 6.

water content may even go up when the vegetation fraction is very large, while it will go down quickly when the ground is nearly bare as showed in Expt. 6. So from the above discussion, we can reach the conclusion that the effect of σ_f is paramount in the variation of Expt. 3 soil water content. The value of w_g and and w_2 in Expt. 3 are greater than those in Expt. 2 because the initial value of soil water content in Expt. 3 is set to be larger than Expt. 2. However, the tendency of two curves are nearly the same, which tells us that albedo and initial water content in the soil have little influence on the variation of water in the soil.

Figure 7 shows the variation of ground surface temperature over the period of one day. We can see that the fluctuation of T_g in Expt. 1 is less than Expts. 2, 3 and 4, and the peak of the maximum at noon in Expt. 1 is the lowest among the first four experiments. This result indicates that vegetation fraction is also the largest influencing factor in the variation of ground surface temperature. Experiments 5 and 6 testify this conclusion by more conspicuous curves. As they show, in Expt. 5, the fluctuation of T_g is the least due to its largest vegetation fraction. On the other hand, the peak of maximum land surface temperature in Expt. 6

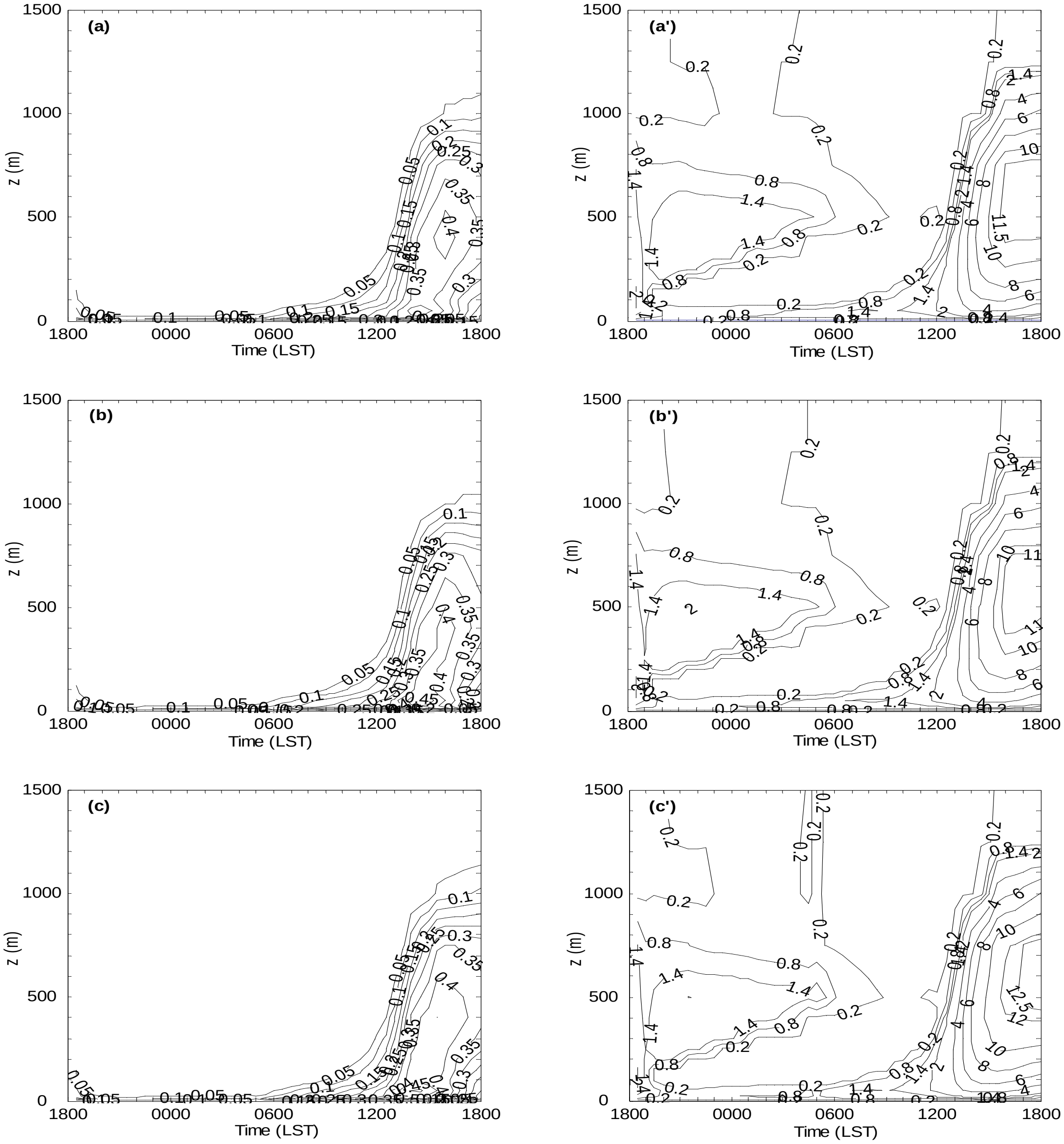

Fig. 8. (Left) Spatial and temporal distribution of turbulence energy (left) exchange coefficient (right). (a) (a') Expt. 1, (b) (b') Expt. 2, (c) (c') Expt. 3, (d) (d') Expt. 4, (e) (e') Expt. 5, and (f) (f') Expt. 6.

nearly arrives at 32°C for little plant covering to protect the ground from the direct radiation of the Sun.

In the following passages, we will discuss the variation of turbulence kinetic energy. The left side of Fig. 8 records the spatial distribution of turbulence energy with the passage of time in the different experiments, and the right side records corresponding turbulence exchange coefficient. The height of all the pictures are from 0 to 1500 m, which is higher than the top of the ML (Mixed Layer) in the ordinary situation. At first, we take a look at the turbulence energy only. The maximum of such energy is 0.4 in Expt. 1, while 0.45 in both Expt. 2 and Expt. 3, 0.50 in Expt. 4, 0.35 in Expt. 5, and 0.95 in Expt. 6. The maximum values are different because of the different values for vegetation fraction designed in the experiments. We can see that the greater the plant cover, the quieter the atmosphere. This is because the vegetation makes the ground rough, which increases ground resistance during the development of turbulence, so the intensity of the eddies refrained. Paying more attention to those pictures, we can find that there is a center at the height of about 100 m in Expts. 2, 3, 4, and 6. However, in Expt. 1 and Expt. 5, the center of turbulence energy

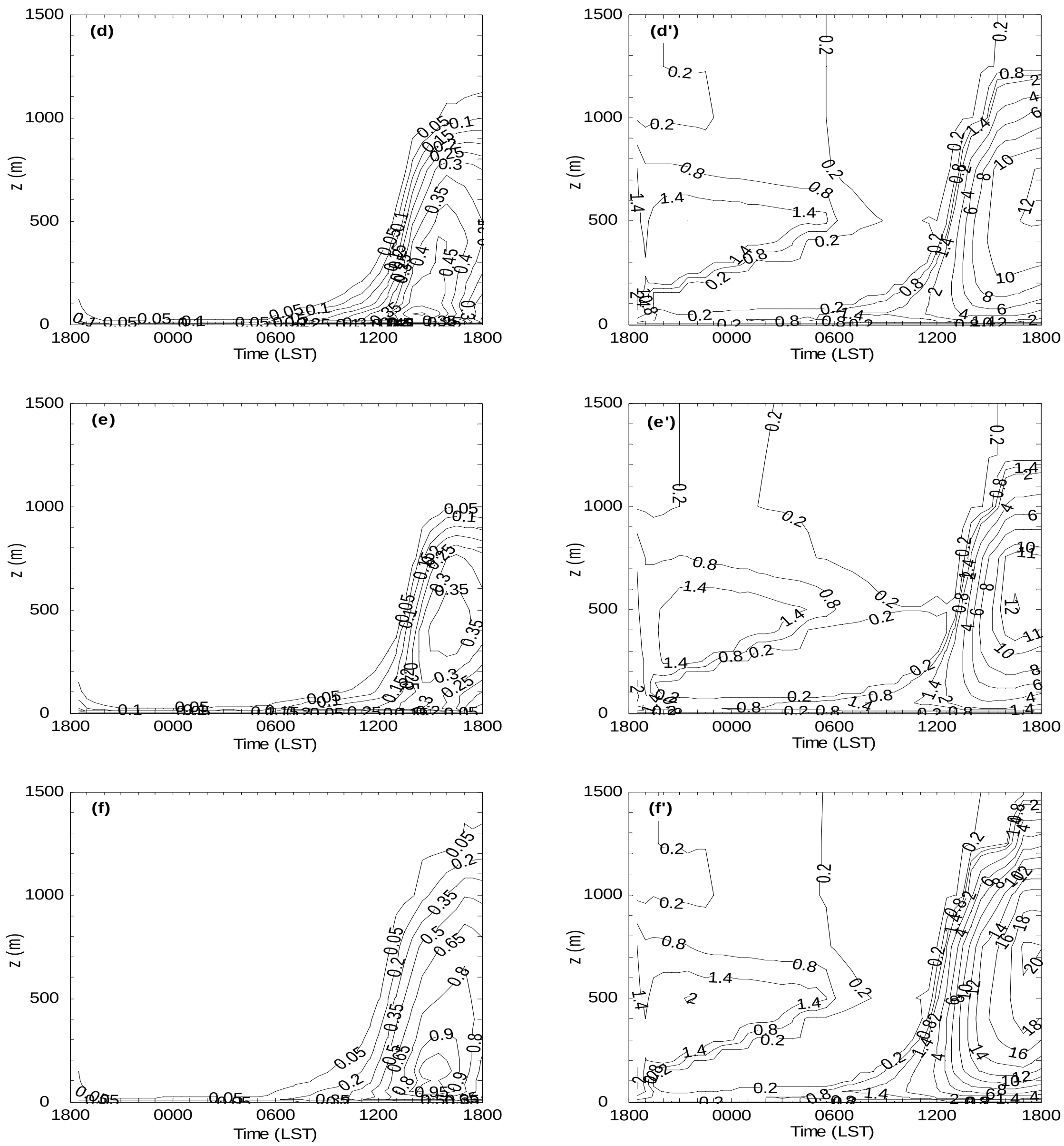

Fig. 8. (Continued)

appears at about 400 m. The reason for this result is that vegetation help to restrain the development of turbulence at low heights. As we know, e^2 (turbulence kinetic energy) is determined by perturbation of velocity, especially of vertical velocity for the uniformity in the horizontal direction. We will find later that the larger the vegetation fraction is, the smaller the vertical velocity near the ground will be. As we know, because w is very small in the synoptic scale, w' is the same magnitude as w. That is why when vegetation fraction is large, the center of turbulence energy will appear to be high. Other information can be obtained from these energy pictures. If we define the isoline whose value is 0.05 as the edge of the eddy, we will clearly see the development of the eddy throughout a whole day. As they show, the height of the NBL (nocturnal boundary layer) is very low at night. However, after the Sun rises, this isoline begins to rise, and will reach a high altitude. This is somewhat like the evolution of the ML. And this line reaches its maximum height at around 18:00. After comparing the result of the six experiments, we find that the altitude of the eddy is the least in Expt. 5 and the largest in Expt. 6. This validates our conclusion that plants can restrain

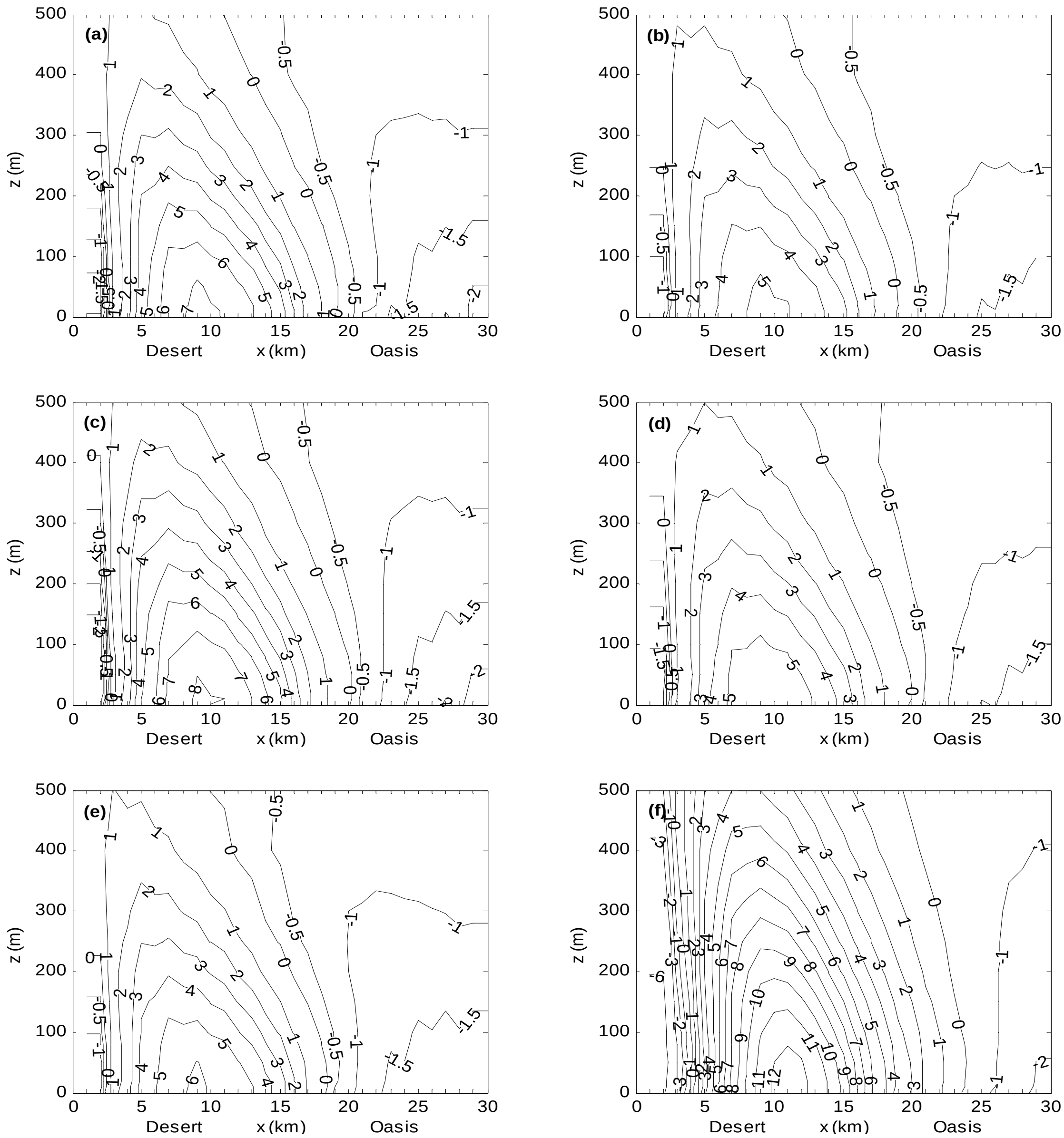

Fig. 9. Spatial distribution of vertical velocity w (cm s^{-1}) at 16:00. (a) Expt. 1, (b) Expt. 2, (c) Expt. 3, (d) Expt. 4, (e) Expt. 5, and (f) Expt. 6.

the development of turbulence. At last, let us look at the variation of the turbulence exchange coefficient shown in the right panels of Fig. 8. Generally speaking, the same regularity is applicable, and no further explanation is needed.

We have just referred to the variation of vertical velocity w, so it needs to be explained here. Figure 9 shows the spatial distribution of vertical velocity at 16:00. First, we look at Expts. 1, 5, and 6, which are just different in the ratio of vegetation cover. As we have said, the land surface causes much hindrance to the movement of the atmosphere when the roughness rises due to a great density of vegetation. So we can see from the figure that the maximum in Expt. 5 is just 6 cm s^{-1}, however, in Expt. 6 it is 12 cm s^{-1}. And the isolines in Expt. 5 are much sparser than the ones in Expt. 6. Now we pay attention to the first four experiments. You may be surprised that the value of center in Expt. 2 and Expt. 4 is less than Expt. 1 and Expt. 3 respectively, though the vegetation factor of the former is larger than the latter. You should not forget that the albedos set in Expt. 2 and Expt. 4 are bigger than the ones in Expt. 1 and Expt. 3. The simulation result tells us that albedo plays an important role in

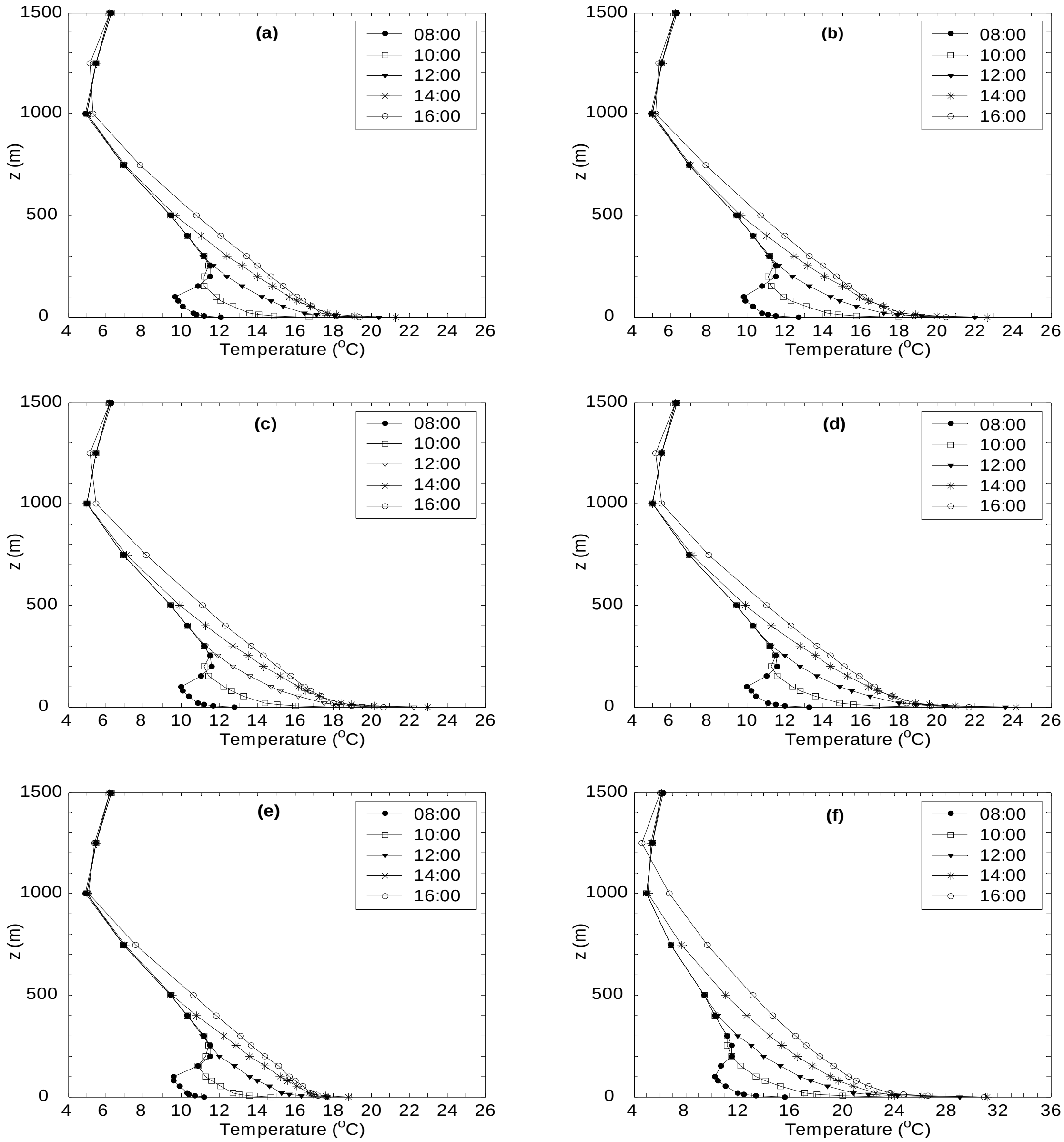

Fig. 10. Temperature profiles at five different times. (a) Expt. 1, (b) Expt. 2, (c) Expt. 3, (d) Expt. 4, (e) Expt. 5, and (f) Expt. 6.

this aspect, which even overpasses the influence brought about by the reduction of vegetation covering.

At the end of the sensitivity experiments, we now look at temperature profiles during daytime. Figure 10 records five profiles in each experiment. We can see from the comparison that the land surface is heated quickly when it is covered by little vegetation. For example, temperature inversion disappears at 10:00 in Expt. 6, while in the other experiments it still exists. Another point we may find out is that lines change slow when $\sigma_{\rm f}$ is great.

At last, we can make several central conclusions from these experiments: the vegetation factor plays a paramount role in the variation of the physical variables, both in the processes of thermodynamics and dynamics. Besides, ground albedo $\alpha_{\rm g}$, foliage albedo $\alpha_{\rm f}$, volume fraction of soil moisture on the ground $w_{\rm g}$, net volume fraction of soil moisture w_2, and $w_{\rm g}$'s saturated value $w_{\rm k}$ also have more or less influence on the physical processes.

3. Summaries and conclusion

This paper uses a Modified Soil-Plant-Atmosphere

Scheme (MSPAS) to simulate land surface processes and boundary layer processes. The stability and sensibility of the model are validated by several sensitivity experiments, which involve the variation of vegetation fraction σ_f, ground albedo α_g, foliage albedo α_f, soil water content w_g and w_2, and so on. Comparisons among the results of the experiments also make valuable conclusions, which are useful in the research work of desertification control in China.

Together with the first paper, we have proved fully that MSPAS is suitable for the study of the interaction between land surface processes and the atmospheric boundary layer in semi-arid regions, and even can be extended for regional climate study. The results from the simulation show practical value in the guidance of desertification control and reforestation in China.

Acknowledgments. This study was supported by the National Natural Science Foundation of China (Grant No. 40275004) and the State Key Laboratory of Atmosphere Physics and Chemistry, and the City University of Hong Kong Grant 8780046, the City University of Hong Kong Strategic Research (Grant No.7001038).

APPENDIX

List of Symbols

e^2 turbulence kinetic energy ($\mathrm{m^2\ s^{-2}}$)
σ_f vegetation fraction
α_f vegetable albedo (0.20)
α_g albedo of ground
q_a specific humidity of the air at the top of canopy ($\mathrm{kg\ kg^{-1}}$)
q_g specific humidity of the ground ($\mathrm{kg\ kg^{-1}}$)
q_f specific humidity of the surface of foliage ($\mathrm{kg\ kg^{-1}}$)
q_af specific humidity of the atmosphere within canopy ($\mathrm{kg\ kg^{-1}}$)
T_g temperature of the ground (K)
T_af temperature of the atmosphere within canopy (K)
w velocity of atmosphere in the vertical direction ($\mathrm{m^2\ s^{-1}}$)
w_g volume fraction of soil moisture on the ground ($\mathrm{m\ s^{-1}}$)
w_2 net volume fraction of soil moisture ($\mathrm{m\ m^{-1}}$)
w_k volume of water hold by soil when the surface acts as if it were saturated ($\mathrm{m\ m^{-1}}$)
w_max maximum volume fraction of soil moisture ($\mathrm{m\ m^{-1}}$)
W_dew interception of water on the foliage when raining ($\mathrm{kg\ m^{-2}}$)

REFERENCES

Bhumralkar, C. M, 1975: Numerical experiments on the computation of ground surface temperature in an atmospheric general circulation model. *J. Appl. Meteor.*, **14**, 67–100.

Blackadar, A. K, 1976: Modeling the nocturnal boundary layer. *Proc. Third Symp. on Atmospheric Turbulence, Diffusion and Air Quality*, Boston, Amer. Meteor. Soc., 46–49.

Bonan, G. B., and A. Land, 1996: Surface Model (LSM Version1.0) for Ecological, Hydrological and Atmospheric Studies: Technical Description and User's Guide. NCAR Technical Note/TN-417+STR, Boulder (Colorado): NCAR,150pp.

Clapp, R. B., 1978: Empirical equations for some soil hydrolic properties. *Water Resour. Res.,* **14**, 601–604.

Charney, J. G., W. Quirk, S. Chow, and J. Kornfield, 1977: A comparative study of the effects of albedo change on drought in semi-arid regions. *J. Atmos. Sci.,* **34**, 1366–1385.

Dan Li, Ji Jinjun, and Li Yinpeng, 2002: Climate simulations based on a different-grid nested and coupled model. *Adv. Atmos. Sci.,* **19**(3), 487–499.

Deardorff, J. W., 1978: Efficient prediction of ground surface temperature and moisture with inclusion of a layer of vegetation. *J. Geophy. Res.,* **83**, 1889–1903.

Dickinson, R. E., A. Henderson-Sellers, and P. J. Kennedy, 1986: Biosphere-Atmosphere Transfer Scheme (BATS) for the NCAR Community Climate Model. NCAR/TN-275+STR. Boulder (Colorado): NCAR.

Dickinson, R. E., A. Henderson-Sellers, and P. J. Kennedy, 1993: Biosphere-Atmosphere Transfer Scheme (BATS) Version 1e as Coupled to the NCAR Community Climate Model. NCAR/TN -387+STR, Boulder (Colorado), NCAR.

Guo Weidong, Sun Shufen and Qian Yongfu, 2002: Case analyses and numerical simulation of soil thermal impacts on land surface energy budget based on an offline land surface model. *Adv. Atmos. Sci.,* 19(2), 500–512.

Liu Shuhua, Huang Zichen, and Liu Lichao, 1997: Numerical simulation of the influence of vegetation cover factor on boundary layer climate in semi-arid region. *Acta Meteorologica Sinica.* **11**, 66–78.

Liu Shuhua, Wen Pinghui, Zhang Yunyan, Hong Zhongxiang, Hu Fei, and Liu Huizhi, 2002: Sensitivity tests of interaction between land surface physical process and atmospheric boundary layer, *Acta Meteorologica Sinica*, **16**, 451–469.

Liu shuhua, Yue Xu, Liu Huizhi, and Hu Fei, 2004: Using a Modified Soil-Plant-Atmosphere Scheme (MSPAS) to simulate the interaction between land surface processes and atmospheric boundary layer in semi-arid region. *Adv. Atmos. Sci.*, **21**(2), 245–259.

Mahfouf, J. F., E. Richard, and P. Mascart, 1987: The influence of soil and vegetation on the development of mesoscale circulations. *J. Climate Appl. Meteor.*, **26**, 1483–1495.

Noilhan, J., and S. Planton, 1989: A simple parameterization of land surface processes for meteorological models. *Mon. Wea. Rev.,* **117**, 536–549.

Sun Shufen, and Xue Yongkang, 2001: Implementing a new snow scheme in simplified simple biosphere model. *Adv. Atmos. Sci.,* **18**(3), 33–354.

Sang Jianguo, and Wu Yidan, 1992: Numerical simulation of atmospheric boundary layer over inhomogeneous underlying surface. *Plateau Meteorology*, **11**(4), 400–410. (in Chinese)

Sellers, P. J., Y. Mintz, Y. C. Sud, and A. Dalcher, 1986: A simple biosphere model (SiB) for use within general circulation models. *J. Atmos. Sci.,* **43**, 505–531.

Sellers, P. J., S. O. Los, and C. J. Tucker, 1996: A revised land surface parameterization (SiB2) for atmospheric GCMs. Part I: Model formulation. *J. Climate,* **9**, 676–705.

Wu Bo, and Lu Qi, 2002: Features of desertification & importance of desertification control in China. *Natural Disaster Reduction in China*, **11**, 141–144.

Zhang Yu, and Lu Shihua, 2002: Development and validation of a simple frozen soil parameterization scheme used for climate model. *Adv. Atmos. Sci.,* **19**(2), 513–527.